Spatiotemporal dynamics of discrete sine-Gordon lattices with sinusoidal couplings

Zhigang Zheng,[1,2,*] Bambi Hu,[1,3] and Gang Hu[4,2]
[1]*Department of Physics and Center for Nonlinear Studies, Hong Kong Baptist University, Hong Kong*
[2]*Department of Physics, Beijing Normal University, Beijing 100875, China*
[3]*Department of Physics, University of Houston, Houston, Texas 77204*
[4]*Center of Theoretical Physics, Chinese Center of Advanced Science and Technology (World Laboratory), Beijing 8730, China*
(Received 13 May 1997)

The spatiotemporal dynamics of a damped sine-Gordon chain with sinusoidal nearest-neighbor couplings driven by a constant uniform force are discussed. The velocity characteristics of the chain versus the external force are shown. Dynamics in the high- and low-velocity regimes are investigated. It is found that in the high-velocity regime, the dynamics is dominated by rotating modes, the velocity shows a branching bifurcation feature, while in the low-velocity regime, the velocity exhibits steplike dynamical transitions, broken by the destruction of strong resonances. [S1063-651X(98)08201-4]

PACS number(s): 03.20.+i, 05.45.+b, 05.40.+j

I. INTRODUCTION

Spatiotemporal dynamics in systems with many degrees of freedom has gained great interest during the last 20 years because of their complicated spatiotemporal patterns and possible applications in many fields, such as turbulence, neural networks, biology, secure telecommunications, spatiotemporal control of chaos, stochastic resonances, Josephson-junction lattices, etc. [1–5]. Research on the discrete sine-Gordon lattice has also seen a surge of interest recently since it can be used to model many physical systems, such as dislocations, magnetic and ferromagnetic domain walls, spin- and charge-density waves, and arrays of Josephson junctions [6,7]. The discrete sine-Gordon chain corresponds to the so-called Frenkel-Kontorova (FK) model in the conservative case, which was mainly studied in exploring the commensurate-incommensurate phase transitions of the ground state [8] and discussing its dc and ac responses [9,10]. Recently, the damped dynamics of this model with harmonic coupling were numerically, theoretically, and experimentally investigated in relating to the fluxon dynamics of one-dimensional Josephson-junction arrays [7,11]. In the damped case, numerous metastable states exist and play a significant role, and this will lead to complicated spatiotemporal patterns and dynamics.

The damped FK chain driven by an external force can be described by the equation of motion of a coupled chain of pendula

$$\ddot{x}_j+\gamma\dot{x}_j+\sin x_j=K[V'(x_{j+1}-x_j-a)-V'(x_j-x_{j-1}-a)]+F, \tag{1}$$

where $V(x)$ describes the coupling law between nearest-neighbor elements, γ, K, a, and F are the friction coefficient, coupling strength, static length of the chain, and the external driving force, respectively. The coupling mechanism of the discrete sine-Gordon chain is generally nonlinear (anharmonic) in the applications to real physical systems. For a real chain of atoms or molecules, the coupling law may be the Lennard-Jones, Toda, or Morse type [12]. For a DNA chain, the couplings of the helices and base pairs are complicated rotator interactions. In the discussions of antiferroelectric liquid crystals, the coupling mechanism of dipoles and layers is also of the sinusoidal form [13]. The nonconvex coupling cases are more interesting than the convex cases. In this paper, we are concerned with the sinusoidal (rotator) coupling case

$$V(x)=1-\cos x. \tag{2}$$

This case is especially realistic when the local degree of freedom is an angle, as in dipolar or magnetic couplings, where $V(x)$ is a periodic function. The sinusoidal coupling is one of the simplest forms. This kind of coupling has been considered for coupled rotator systems [14], base pair rotations in DNA [13], magnetic Heisenberg models [15] and the one-dimensional (1D) chiral XY model [16], granular superconductors [17], and Josephson-junction array ladders [18]. Moreover, for strong-coupling strengths, the sinusoidal interaction can be approximated by the harmonic form. In Fig. 1, two kinds of couplings are shown. Only in the vicinity of the equilibrium position will the two kinds of couplings coincide. It is very interesting to note that these two cases reduce to the same sine-Gordon equation in the continuum limit. In fact, there is not a unique way to discretize a continuum equation. Sometimes nonlinear approaches are more significant because nonlinear localized modes are intrinsically discrete. Therefore it is necessary to study nonlinear coupling cases as they may correspond to some real physically discrete systems.

This paper is organized as follows. In Sec. II we discuss the dynamics in the high-velocity regime. We observe that in this regime, rotating modes dominate, as theoretically predicted [19,20]. The rotating modes result in a branching bifurcation of the v-F (where v is the average velocity of the chain) relation. In Sec. III, the dynamics in the low-velocity regime is analyzed. Dynamical transitions between resonant steps are investigated, and these steps can be theoretically

*Electronic address: zgzheng@public2.bta.net.cn.

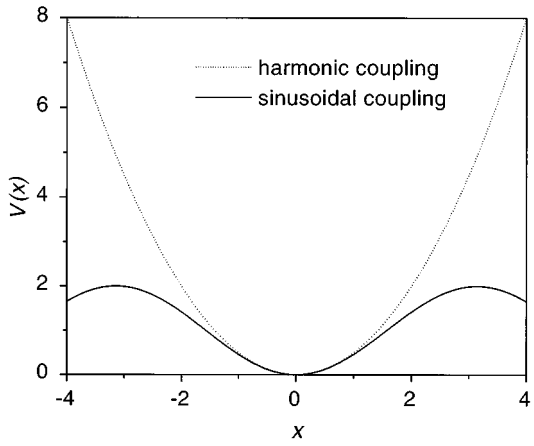

FIG. 1. A schematic plot of two kinds of coupling forms, $V(x)=\frac{1}{2}x^2$ and $V(x)=1-\cos(x)$. Only in a small region near the origin do the two functions coincide.

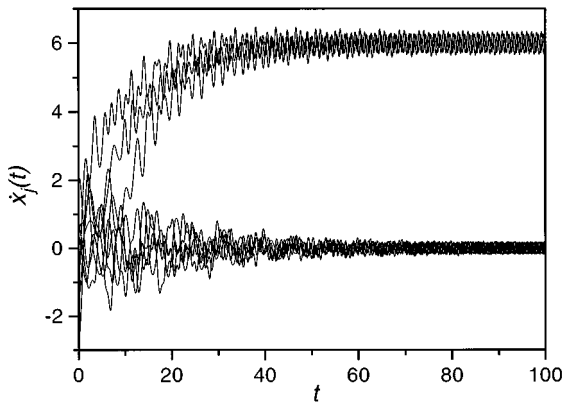

FIG. 2. The evolution of the velocities of an eight-particle system with the sinusoidal coupling. Rotating modes ($v>0$) emerge due to the nonconvexity of the coupling. Both the rotating and pinned particles are oscillatory.

predicted by using the harmonic-coupling formula proposed in [11]. We also find that some steps disappear due to the destruction of traveling-wave solutions. This leads to the emergence of new dynamical phases. Section IV gives some concluding remarks.

II. HIGH-VELOCITY REGIME: ROTATING MODES

By inserting $V(x)=1-\cos x$ into Eq. (2), we rewrite the equation of motion:

$$\ddot{x}_j+\gamma\dot{x}_j+\sin x_j=K[\sin(x_{j+1}-x_j-a)-\sin(x_j-x_{j-1}-a)]+F. \tag{3}$$

This equation is highly nonlinear. Only in some limit cases, for example, $K\to\infty$, can it be analytically treated. Hence we study its dynamics mainly by using numerical simulations. The fourth-order Runge-Kutta integration algorithm is used and the time step is adjusted according to the numerical accuracy. Periodic boundary conditions are added, i.e., $x_{j+N}(t)=x_j(t)+2\pi M$, where M is an integer that counts the net number of kinks trapped in the ring. Therefore the frustration $\delta=M/N$ and the spring constant $a=2\pi\delta$.

In the case of large coupling K, the system can be well described by the continuum sine-Gordon chain. In this case, it was found that there exists a critical chain velocity $v_c=2\pi\delta\sqrt{K}$ that separates two kinds of dynamics (kinks) [21,22]. When $v<v_c$, the motion is that of localized solitons, which is called the *low-velocity regime*. When $v>v_c$, the motion is characterized by a whirling wave, i.e., the moving kink is strongly extended. We call this region the *high-velocity regime*. Let us first study the dynamics in the high-velocity regime. Figure 2 gives a typical evolution of the velocities for an eight-particle chain. It has been found that although there are couplings between the elements, their motions are inhomogeneous; i.e., some particles rotate with a finite velocity while others remain pinned in the potential wells. This is a consequence of both nonconvex coupling and bistability. Recalling the phase-space structure of a single pendulum in the underdamped case, one finds that there are two kinds of attractors with one fixed point and the other running solutions. This leads to bistability [23]. However, distinct difference between the single-particle and sinusoidal-coupling cases can be found in Fig. 2. It is shown that oscillation occurs for both rotating and pinned particles, which is the result of coupling, and this will not happen for the single-particle case. Our numerical picture also supports the prediction of Takeno and Peyrard [19], who proved the existence of the rotating mode in the conservative sinusoidal-coupled sine-Gordon chain. This was also related to what is discussed in [20]. The existence of rotating modes is a consequence of the particular topology of the sinusoidal coupling, which is also a localized excitation like breathers.

In Fig. 3, we plot the average velocity v versus the external driving force F for $N=8$, $K=1$, and $M=1,2,3$. It can be seen that, in the high-velocity regime, there is a bifurcation of v branches, where each branch can be expressed by

$$v_i(t)=v_i^0+\delta v_i\sin(\omega t+\varphi_i), \tag{4}$$

where v_i^0 describes the rotating frequency of the ith particle, the second term corresponds to the oscillation around the central frequency, and δv_i, ω, and φ_i are the oscillation amplitude, the oscillating frequency, and the phase, respectively. The rotating frequency can be expressed by

$$v_i^0=\begin{cases}0 & \text{for a pinned particle}\\ F/\gamma & \text{for a rotating particle.}\end{cases} \tag{5}$$

Thus the average velocity (averaged over time and lattice) will be a quantized one:

$$v=\frac{nF}{N\gamma}, \tag{6}$$

which corresponds to the numerical branches, where $n=1,\ldots,N$. Each numerical point is obtained by starting from randomly chosen initial motions of the chain. The dotted lines are theoretical results (6). One can find that they agree precisely with the numerical results. The mechanism behind this quantization is due to the nonconvexity of the coupling. This leads to many metastable states. It can also be observed from Fig. 3 that, for $M>1$, the bottom few lines

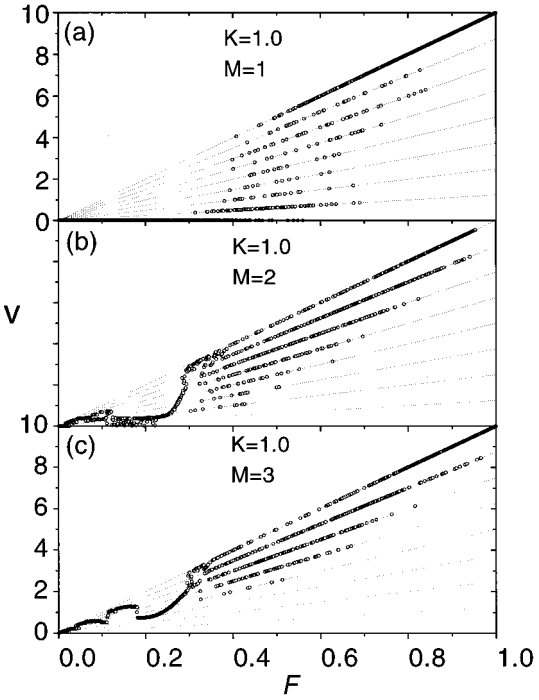

FIG. 3. The v-F characteristics of the sinusoidal coupling cases for $N=8$, $\gamma=0.1$, $K=1.0$, and $M=1,2,3$. Branching bifurcations are shown in the high-velocity regime. Resonance-step transitions can also be observed in the low-velocity regime.

disappear. This is a consequence of multikinks. The threshold forces for emergences of different lines are not the same. Lines with larger slopes have larger threshold values. For the $n=1$ branch, the threshold F_c is just the threshold of the emergence of bistability for a single driven damped pendulum. This is also the smallest threshold.

The rotating modes are stable only for the weak coupling case. If one increases the coupling strength K, the dynamics approaches that of a convex-coupling case. In Fig. 4, we give the v-F characteristics for $N=8$, $M=1$, and $K=5,10$. It can be found that branches of $n<N$ disappear; only the $n=N$ branch survives, i.e., all particles in the chain will rotate. This is natural when one uses a larger coupling strength, because stronger couplings will cause the rotating modes to become unstable. The convex part will strongly affect the rotating modes. It should also be noted that several unstable regions can be observed on the high-velocity line. These regions become smaller when one increases F. This is a residual effect of sinusoidal coupling, where the nonconvex effect can still play a role. In Fig. 5, evolutions of velocities for one of the particles in these regions are shown. We find that motions in small-F unstable regions are irregular while they are complicated periodic or quasiperiodic motions in larger-F unstable regions.

One may also observe the dynamics in the low-velocity regime in the above figures. They are more interesting. Hence we now turn our discussion to dynamics in this region.

III. LOW-VELOCITY REGIME: RESONANT-STEP DYNAMICAL TRANSITIONS

For a sine-Gordon chain with harmonic coupling, dynamics in the low-velocity regime exhibit soliton behavior. But

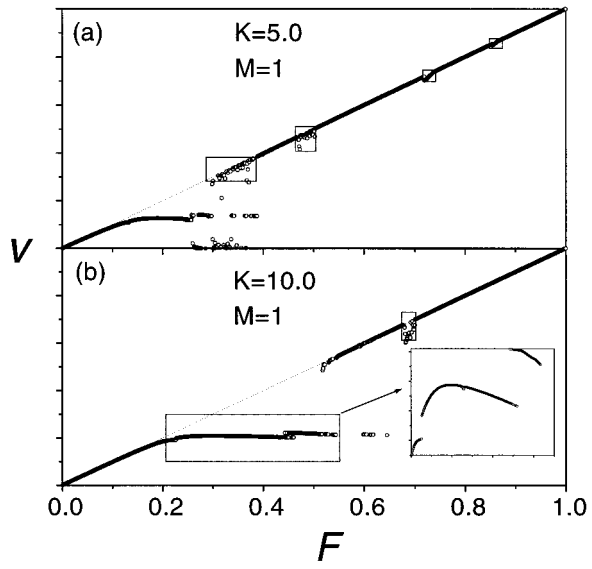

FIG. 4. The v-F plot for $M=1$, $K=5.0$, and 10.0. Other parameters are the same as Fig. 3. Rotating modes are destroyed due to the role of convex part of the coupling. Several unstable regions resulting from the nonconvex effect are labeled by boxes.

because of the discreteness of the chain, the attractor in this region is a distorted traveling wave, which is composed of a moving kink and small superimposed oscillating wave. This will cause the radiation of a small linear wave of a moving

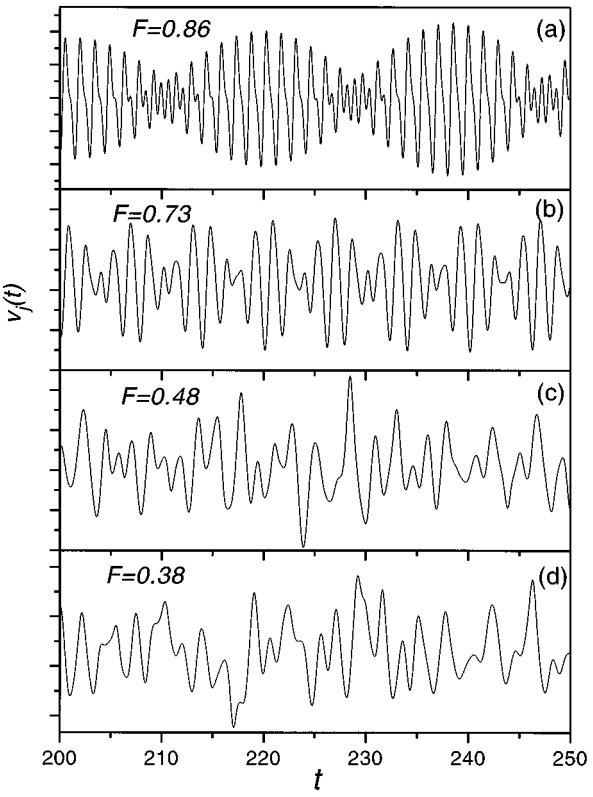

FIG. 5. The motion of one particle in the unstable boxes of Fig. 4(a). Quasiperiodic motion can be observed for smaller forces. In the unstable regions with larger forces, the motion is modulated periodic.

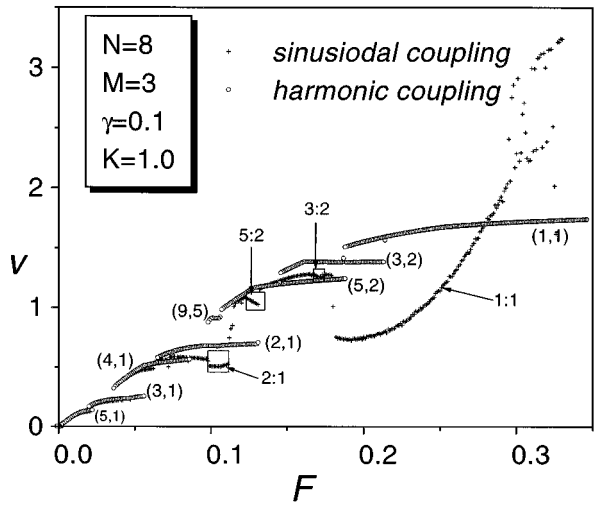

FIG. 6. The v-F relations for both harmonic (circles) and sinusoidal (crosses) cases with the same parameters: $N=8$, $M=3$, $K=1.0$, and $\gamma=0.1$. Step transitions can be observed, and all steps for the harmonic-coupling case are labeled by resonances (m_1,m_2). Good agreement is shown for small forces. Giant steps that are destroyed completely or in part are labeled by boxes (the 1:1 resonance is completely destroyed, hence it is not labeled). The destroyed branches are disordered phases.

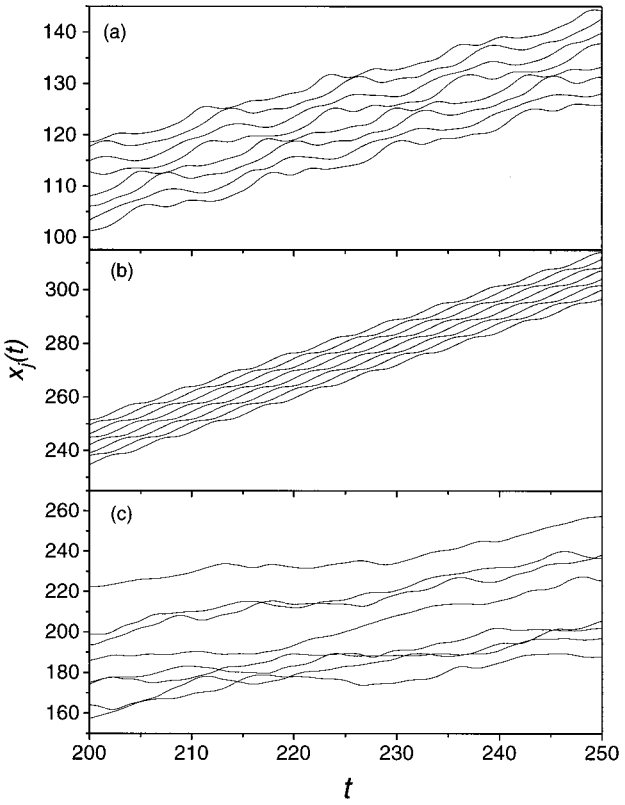

FIG. 7. The evolution of $x_j(t)$ for ordered and disordered phases. The motion on the ordered step is quite a good traveling wave, while the motion is irregular and even chaotic in disordered phases.

kink in its wake. We have given a mean-field description of soliton dynamics in this regime and theoretically predicted the resonance behavior [11].

In the sinusoidal coupling case, similar behaviors only occur for a system with multikinks ($M>1$). In Fig. 3 for $M=1$, we find that in the low-velocity regime, the velocity remains zero; i.e., the chain remains pinned until the external force exceeds a critical value that indicates the emergence of bistability. When one increases the coupling strength K, we find distinct differences, i.e., steplike resonances occur (see Fig. 4, $K=5,10$), which is similar to the harmonic case. In fact, the convex part of the coupling takes effects in this case. On the other hand, nonconvex effects can still play a role in some regimes. For example, in Fig. 4(a), near the boundary between the high- and low-velocity regimes, nonconvex coupling effects are significant, the zero velocity branch reappears. Also in Fig. 4(b) (inset), the enlarged plot of a step shows a negative slope and a small unstable gap can be observed. Figures 3(b) and 3(c) show the situations for $M>1$. Dynamics in the low-velocity regime is rather complicated. In Fig. 3(b), for $M=2$, the depinning force F_c is very small, and zero velocity reappears around 0.1 to 0.2. This is also a nonconvex effect.

In Fig. 6, we enlarge the low-velocity regime of Fig. 3(c) for $M=3$ in order to give a more precise analysis. In order to make a good comparison, we also plot the v-F curve for the harmonic case where all parameters remain the same as the sinusoidal case. For both cases, steplike dynamical transitions can be observed. Transitions between these states lead to the gaps in Fig. 6. We studied the mechanisms of the gap behavior for the harmonic case. The existence of resonance steps is a time-scale competition between kink propagation and its radiated phonon waves. When the two frequencies satisfy the resonance condition, the mode is locked; hence steps occur. We have derived a formula for all the steps [11]:

$$v(m_1,m_2)=\frac{m_2}{m_1}\sqrt{\beta+4K\sin^2\left(\frac{m_1\delta\pi}{m_2}\right)}, \qquad (7)$$

where (m_1,m_2) is a pair of integers that describes the resonance between kinks and linear waves, δ is the frustration, and β is a contraction factor that we introduced in terms of mean-field treatment to consider the commensurability effect. Physically β can be interpreted as the depinning force that is needed to overcome the Pierels-Nabarro (PN) barrier and continuously move the static kink along the chain [11]. Steps in Fig. 6 can be well recognized by using Eq. (7) and all resonance steps are labeled for the harmonic case. It may be found that for a small force, steps for the sinusoidal case can exist and agree well with those for the harmonic case. However, there are several regions where the velocity jumps down to a lower branch. This kind of dynamical transition did not occur for the harmonic coupling case; hence this is also a typical nonconvex effect. A careful comparison between these two cases indicates that *these dropoffs correspond to the destruction of strong resonances*. The most significant step that is completely destroyed is the 1:1 resonance, where the traveling-wave solution becomes unstable. In addition, 2:1, 3:2, and other giant resonance steps are also partly destroyed. In Fig. 7, we give the evolution of $x_i(t)$ in the destructed regions. A typically good traveling wave is also shown in order to make a comparison. It is

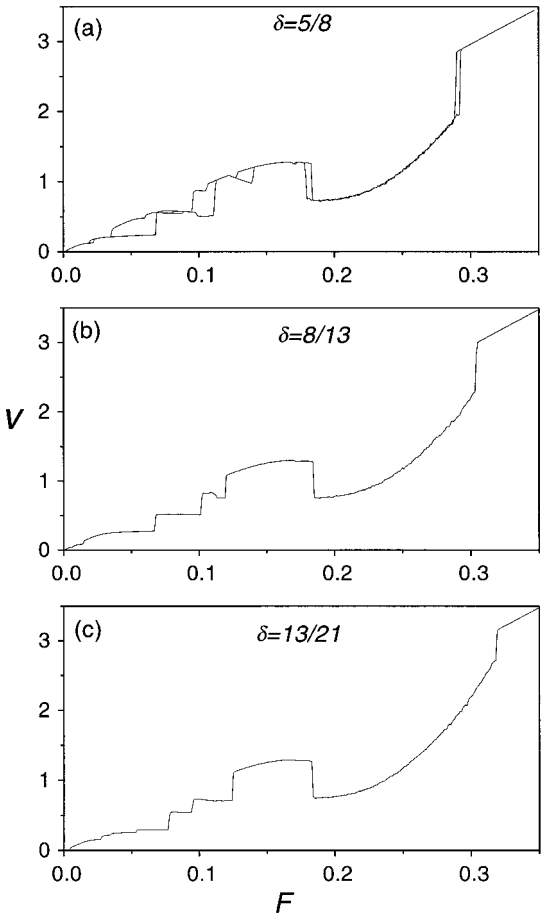

FIG. 8. The v-F characteristics for the approach to golden mean $\delta_G=(\sqrt{5}-1)/2$ via the Fibonacci sequence $\delta=\frac{5}{8}, \frac{8}{13}, \frac{13}{21}, \ldots$. The disordered phase 1:1 can always be observed.

vividly observed that in the resonance-destructed regions, the traveling wave becomes unstable and disordered motion takes place. This can be qualitatively understood. While the kink frequency and its linear wave satisfy the resonance condition, for those strong enough resonances, they are so strong that the linear wave around the kink becomes unstable and is amplified, this will in turn destroy the traveling wave, and eventually the dynamics becomes chaotic and resonant steps disappear. The 1:1-destructed region is a typical chaotic region, and this also leads to the connection between low- and high-velocity regimes. We call the 1:1 branch a *disordered phase*. Numerical studies indicate that the motion on this whole branch is chaotic, and the preserved order is completely destroyed.

It is very interesting to note that this mechanism is valid especially for incommensurate cases. For example, when δ is the golden mean $\delta_G=\sqrt{5}-1/2$, the 1:1 resonance will always be destroyed for intermediate coupling cases, i.e., the disordered phase always exists. This is another route for the transition between low- and high-velocity regimes, which occurs only for nonconvex cases. In Fig. 8, we give the v-F characteristics of the golden mean approach by the Fibonacci sequence $\delta=\frac{5}{8}, \frac{8}{13}$, and $\frac{13}{21}, \ldots$; it can be easily found that at $F_c\simeq 0.318$ the chain velocity always drops to the lower disorder phase, where the 1:1 resonance causes the traveling wave to be unstable.

IV. CONCLUDING REMARKS

In this paper, we have studied the dynamics of the discrete sine-Gordon chain with a sinusoidal coupling. Complicated spatiotemporal patterns exist in this nonlinear lattice system. In the high-velocity regime, the attractors are the rotating waves. The motion of the chain may be inhomogeneous, i.e., some particles can remain pinned while others rotate. This is a consequence of both nonconvex discreteness and bistability. This inhomogeneity leads to a branching bifurcation of the v-F characteristics. For stronger couplings, branching bifurcation is destroyed and only the collective motion branch survives. A nonconvex effect still can be observed along this branch. In the low-velocity regime, the attractor in a large region is the traveling wave. This is similar to the harmonic-coupling case, where the convexity of the interaction leads to traveling-wave propagation. Resonant-step transitions can be well predicted by the formula (7). However, due to the intrinsic nonconvexity of the sinusoidal coupling, some resonant steps are completely or partly destroyed, leading to the disordered phase. This causes the traveling wave to be unstable, hence the motion becomes irregular and even chaotic.

The present model and results may be applied to some experimental fields, such as granular superconductors and Josephson-junction ladders. In the experimental studies of the discrete Josephson transmission lines with stacked junctions [24] and coupled long Josephson junctions [25], similar behaviors also exist. Moreover, oscillating breathers and rotating states have also been found. In the investigation of Josephson-junction ladders [26], the same coupling model corresponding to the 1D chiral XY model has been proposed [16]. The ground state and relaxation phenomena had been fully explored. But to our knowledge, no discussions on the damped driven dynamics of this model have been found. In a real experimental environment, such considerations may give more insight into the intrinsic properties of the system. The present work may be a first step in exploring the spatiotemporal behaviors in this model. Moreover, much knowledge can be captured in the investigation of this kind of disorder system, compared to the continuum sine-Gordon system. An important issue concerns the noise effect in this system, for fluctuations will induce transitions between different dynamical states. This problem is now under exploration.

ACKNOWLEDGMENTS

One of the authors (Z.Z.) thanks Professor David Stroud and Professor N. M. Plakida for useful discussions on superconductivities and Josephson-junction arrays and Professor L. H. Tang for discussions on the ground-state problem. This work was supported in part by the Research Grant Council RGC and a Hong Kong Baptist University faculty research grant (FRG).

[1] Y. Kuramoto, *Chemical Oscillations, Waves and Turbulence* (Springer-Verlag, New York, 1984).
[2] A. T. Winfree, *The Geometry of Biological Time* (Spring-Verlag, New York, 1980).
[3] K. Kaneko, Phys. Rev. Lett. **63**, 219 (1989); Physica D **55**, 368 (1992); Chaos **2**, No. 2 (1992), special issue on spatiotemporal chaos.
[4] Gang Hu and Zhilin Qu, Phys. Rev. Lett. **72**, 68 (1994). For spatiotemporal stochastic resonances, see the following papers: Gang Hu, H. Haken, and F. Xie, Phys. Rev. Lett. **77**, 1925 (1996); F. Marchesoni, L. Gammaitoni, and A. R. Bulsara, *ibid.* **76**, 2609 (1996); J. Linder, B. Meadows, and W. Ditto, Phys. Rev. E **53**, 2081 (1996); J. Linder, B. Meadows, W. Ditto, M. Inchiosa, and A. R. Balsara, Phys. Rev. Lett. **75**, 3 (1995); P. Jung and G. Mayer-Kress, *ibid.* **74**, 2130 (1995); M. Locher, G. Johnson, and E. Hunt, *ibid.* **77**, 4698 (1996).
[5] K. Wiesenfeld, P. Colet, and S. Strogatz, Phys. Rev. Lett. **76**, 404 (1996).
[6] M. Remoissenet, *Wave Called Solitons, Concepts and Experiments* (Springer-Verlag, Berlin, 1994).
[7] S. Watanabe, H. Zant, S. Strogatz, and T. Orlando, Physica D **97**, 429 (1996); H. van der Zant, T. Orlando, S. Watanabe, and S. Strogatz, Phys. Rev. Lett. **74**, 174 (1995); A. Ustinov, M. Cirillo, and B. Malomed, Phys. Rev. B **47**, 8357 (1993); A. V. Ustinov, M. Cirillo, B. Larsen, V. A. Gbozunov, P. Carelli, and G. Rotoli, *ibid.* **51**, 3081 (1995).
[8] S. Aubry, Phys. Rep. **103**, 12 (1984).
[9] S. Coppersmith, Phys. Rev. B **30**, 410 (1984); S. Coppersmith and D. Fisher, Phys. Rev. A **38**, 6338 (1988); L. Sneddon and K. Cox, Phys. Rev. Lett. **58**, 1903 (1987); L. Sneddon, S. Liu, and A. J. Kassman, Phys. Rev. B **43**, 5798 (1991).
[10] L. Floria and F. Falo, Phys. Rev. Lett. **68**, 2713 (1992); F. Falo, L. Floria, P. Martinez, and J. Mazo, Phys. Rev. B **48**, 7434 (1993); J. Mazo, F. Falo, and L. Floria, *ibid.* **52**, 6451 (1995); for recent reviews on dissipative dc and ac dynamics in FK model, see L. Floria and J. Mazo, Adv. Phys. **45**, 505 (1996).
[11] Zhigang Zheng, Bambi Hu, and Gang Hu (unpublished).
[12] I. Markov and A. Trayanov, J. Phys. C **21**, 2475 (1988); B. Lin and B. Hu, J. Stat. Phys. **69**, 1047 (1992).
[13] S. Takeno and S. Homma, J. Phys. Soc. Jpn. **59**, 1890 (1990); **55**, 2547 (1986); X. Y. Wang and P. L. Taylor, Phys. Rev. Lett. **76**, 640 (1996).
[14] S. Kim, S. Park, and C. Ryu, Phys. Rev. Lett. **78**, 1616 (1997); H. Takana, A. Lichtenberg, and S. Oishi, *ibid.* **78**, 2104 (1997); K. Tsang and K. Nagi, Phys. Rev. E **54**, R3067 (1996); J. Rogers and L. Wille, *ibid.* R2193, 54 (1996); S. Strogatz, R. Mirollo, and P. Matthews, Phys. Rev. Lett. **68**, 2730 (1992); H. Daido, *ibid.* **77**, 1406 (1996); **78**, 1683 (1997).
[15] M. Antoni and S. Ruffo, Phys. Rev. E **52**, 2361 (1995).
[16] C. Yokoi, L. Tang, and W. Chou, Phys. Rev. B **37**, 2173 (1988).
[17] R. Fishman and D. Stroud, Phys. Rev. B **38**, 290 (1988).
[18] S. Ryu, W. Yu, and D. Stroud, Phys. Rev. E **53**, 2190 (1996); B. Kim, S. Kim, and S. Lee, Phys. Rev. B **51**, 8462 (1995); J. Kim, W. Choe, S. Kim, and H. Lee, *ibid.* **49**, 459 (1994); C. Denniston and C. Tang, Phys. Rev. Lett. **75**, 3930 (1995).
[19] S. Takeno and M. Peyrard, Physica D **92**, 140 (1996); Phys. Rev. E **55**, 1922 (1997).
[20] R. S. Mackay and S. Aubry, Nonlinearity **7**, 1623 (1994).
[21] Y. Kivshar and B. Malomed, Rev. Mod. Phys. **61**, 763 (1989).
[22] D. McLaughlin and A. Scott, in *Solitons in Action*, edited by K. Lonngren and A. Scott (Academic Press, New York, 1978).
[23] H. Risken, *The Fokker-Planck Equation, Methods of Solution and Applications* (Springer-Verlag, Heidelberg, 1984).
[24] P. Caputo, M. Darula, A. Ustinov, and H. Kohlstedt, J. Appl. Phys. **81**, 309 (1997).
[25] S. Hattel, A. Grunnet-Jepsen, and M. Samuelsen, Phys. Lett. A **221**, 115 (1996).
[26] J. Mazo, F. Falo, and L. Floria, Phys. Rev. B **52**, 10 433 (1995).